Size distribution of percolating clusters on cubic lattices

2000 J. Phys. A: Math. Gen. 33 7687

(http://iopscience.iop.org/0305-4470/33/43/302)

J. Phys. A: Math. Gen. **33** (2000) 7687–7697. Printed in the UK PII: S0305-4470(00)13722-9

Size distribution of percolating clusters on cubic lattices

Jean-Christophe Gimel, Taco Nicolai and Dominique Durand

Polymères, Colloïdes, Interfaces, UMR CNRS, Université du Maine F-72085 Le Mans cedex 9, France

E-mail: jean-christophe.gimel@univ-lemans.fr

Received 6 April 2000

Abstract. We present Monte Carlo simulations of site percolation on cubic lattices with size L. The cut-off function of the size distribution at the characteristic size s^* can be described by a Gaussian for site occupations (p) lower than the critical value for percolation (p_c) while for $p > p_c$ it is better described by a stretched exponential. Finite lattice size effects depend on both $\varepsilon = (p_c - p)/p_c$ and L and cannot be eliminated by normalization with the distribution at $\varepsilon = 0$. We give a general expression of the cut-off function valid for any ε sufficiently small and L sufficiently large. Using this general expression, we calculate the finite lattice size effects on the weight average (s_w) and z-average (s_z) sizes which are in good agreement with values directly obtained from the simulations.

1. Introduction

Two decades ago it was suggested [1] that gelation caused by random aggregation of molecules, polymers or colloids can be described as a percolation process close to the gel point. Percolation in three dimensions cannot be resolved analytically and has therefore been investigated using Monte Carlo simulations; see [2] for a review. It was found that large percolating clusters have a fractal structure so that

$$s \propto R^D \qquad s \gg 1 \tag{1}$$

where s is the number of sites of the cluster with characteristic radius R, and D is the so-called fractal dimension. The number of clusters per site with size s has a power law dependence on s:

$$N(s) = f_{\text{int}}(s)\, s^{-\tau}\, f_{\text{ext}}(s/s^*) \tag{2}$$

where $f_{\text{int}}(s)$ is the internal cut-off function which is constant for $s \gg 1$ and $f_{\text{ext}}(s/s^*)$ is the external cut-off function at a characteristic size s^* which is unity for $s \ll s^*$ and decreases faster than a power law for $s \gg s^*$. f_{ext} is also called the scaling function and f_{int} the correction to scaling. s^* diverges at the percolation threshold as

$$s^* \propto |\varepsilon|^{-1/\sigma} \quad \varepsilon \to 0 \tag{3}$$

with $\varepsilon = (p_c - p)/p_c$, where p is the probability that a site is occupied and p_c is the critical value at the percolation threshold. p_c depends on the details of the lattice used in the simulation ($p_c = 0.3116$ for site percolation on a simple cubic lattice). On the other hand, the exponents D, τ and σ are expected to depend only on the spatial dimension, and not on the details of the lattice. Precise values have recently been established in three dimensions [3, 4, 5, 6]:

0305-4470/00/437687+11$30.00

$D = 2.53$, $\tau = 2.19$ and $\sigma = 0.45$. The functional form of $N(s)$ does not depend on ε except that f_{ext} is different for $\varepsilon > 0$ and $\varepsilon < 0$.

Subsequent experimental work showed that many characteristics of real gelling systems were consistent with computer simulations of the percolation model. But both the computer simulations and the experiments were mainly focused on scaling laws ignoring the problem of the limits to the scaling behaviour. However, as we have shown elsewhere [7], ignoring the influence of the cut-off functions can lead to significant errors in the determination of the exponents. The only way to avoid this error is to consider the cut-off functions explicitly, which in addition gives a more complete description of the experimental results.

Recently [8], we reported Monte Carlo simulations of site percolation in three dimensions and gave a more accurate expression for f_{ext} at $p < p_c$ than was available at the time. We compared the simulation results with the experimentally observed molar mass distributions of gelling systems reported in the literature. In that work we avoided finite lattice size effects by extrapolation to lattice size $L \to \infty$. Here we want to address the influence of finite size effects. We will use the results to calculate the finite size effect on the weight averaged (s_w) and z-averaged (s_z) sizes of the percolating clusters, which are the reduced second and third moment of the distribution:

$$s_w = \frac{1}{p} \int_1^\infty s^2 N(s)\, \mathrm{d}s \tag{4}$$

$$s_z = \frac{\int_1^\infty s^3 N(s)\, \mathrm{d}s}{\int_1^\infty s^2 N(s)\, \mathrm{d}s} \propto s^*. \tag{5}$$

We will also give an expression for f_{ext} and f_{int} valid for any ε sufficiently small and L sufficiently large.

2. Results

We have performed Monte Carlo simulations of site percolation on simple cubic lattices with free boundary conditions and using the so-called Hoshen and Kopleman algorithm [9]. The results were averaged over a large number of trials in order to reduce the standard error to less than 1% (more than 10 000 trials are needed for $\varepsilon = 0$ while 500 are sufficient for $|\varepsilon| = 0.1$).

Figure 1 shows the size distributions at different L for a given value of ε. For a given value of s, $N(s, \varepsilon, L)$ has a linear dependence on L^{-1} at large L as was found earlier for percolation in two dimensions [10]. The range of linearity decreases with increasing s which renders the use of large lattices necessary at large s. Using lattices with L up to 1023, the smallest ε for which $N(s)$ can be determined accurately over the whole range of s is about 6×10^{-3}. The values extrapolated to $L \to \infty$ are indicated in figure 1 by a dashed line.

Figure 2 shows the size distributions at different ε before and after the gel point obtained after extrapolation to $L \to \infty$. The dashed line in figure 2 indicates the limiting power law behaviour: $N(s) = k_1\, s^{-\tau}$ with $k_1 = 0.069$ and $\tau = 2.19$. The deviation at small s is caused by the internal cut-off. It has been postulated [11] that the internal cut-off function has the following form:

$$f_{\text{int}}(s) = k_1\, (1 + k_2\, s^{-\Omega}). \tag{6}$$

In figure 3 we have plotted $k_1 - s^\tau N(s, 0, \infty)$ as a function of s at $\varepsilon = 0$ for $L \to \infty$. We have added for $s \leqslant 12$ exact values obtained from enumeration of lattice animals [12, 13],

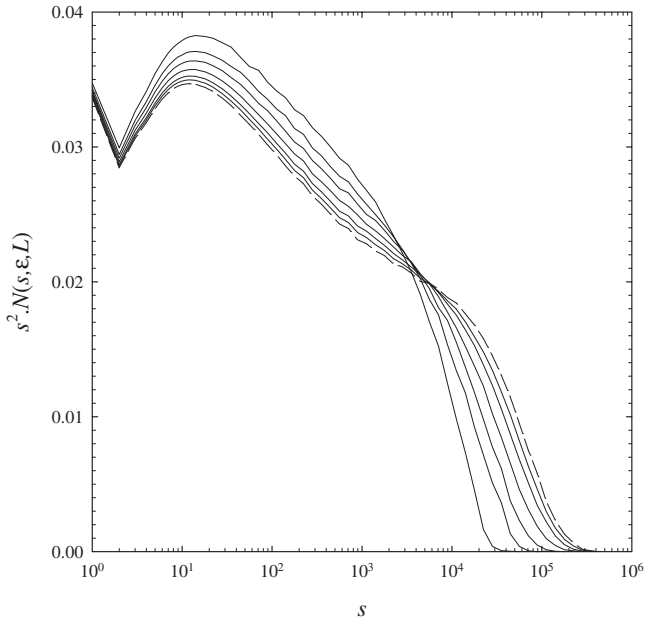

Figure 1. $s^2\,N(s,\varepsilon,L)$ as a function of s at $\varepsilon = 8.66 \times 10^{-2}$ and $L = 84$, 124, 174, 276, 511 and 1023. The dashed line is the extrapolation at $L \to \infty$.

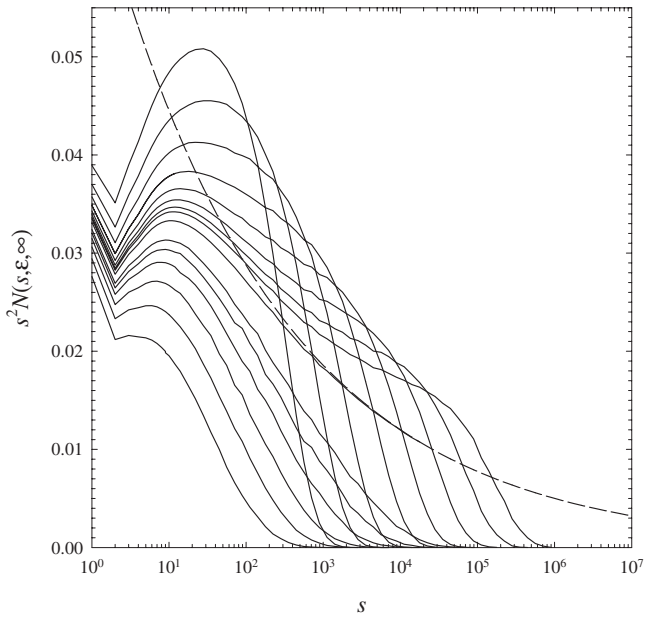

Figure 2. $s^2\,N(s,\varepsilon,\infty)$ as a function of s at various ε: before the gel point ($5.78 \times 10^{-3} \leqslant |\varepsilon| \leqslant 1.00 \times 10^{-1}$), after the gel point ($1.32 \times 10^{-2} \leqslant |\varepsilon| \leqslant 1.00 \times 10^{-1}$) and at the gel point ($\varepsilon = 0$). From the top to the bottom the solid lines correspond to $p = 0.2804$, 0.2908, 0.2976, 0.3024, 0.3054, 0.3075, 0.3089, 0.3098, 0.3116, 0.3157, 0.3178, 0.3208, 0.3256, 0.3324 and 0.3428. The dashed line represents the asymptotic power law behaviour at $p = p_c$.

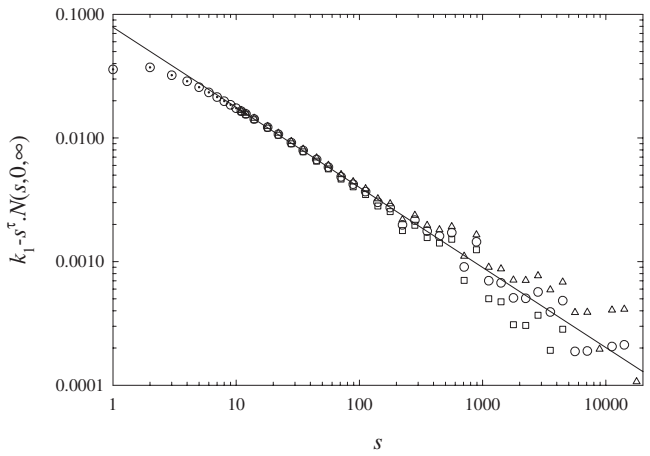

Figure 3. $k_1 - s^\tau N(s, 0, \infty)$ as a function of s at the gel point, using $\tau = 2.19$ and various k_1: 0.0690 (circles,) 0.0688 (squares) and 0.0692 (triangles). The dots represent exact results from enumeration of lattice animals. The solid line represents a linear least squares fit to the data for $10 \leqslant s \leqslant 100$.

which are in excellent agreement with our simulation results. In this representation equation (6) predicts a linear dependence on s with intercept k_1k_2 and slope $-\Omega$. We have fixed τ at the accurate literature value and varied k_1. The best linear dependence was obtained using $k_1 = 0.0690$ with a visually estimated error of ± 0.0002. A linear least squares fit to the data for $10 \leqslant s \leqslant 100$ gives $\Omega = 0.65 \pm 0.02$ and $k_2 = -1.13 \pm 0.02$, where the errors represent the 95% confident interval. Recently, Lorenz and Ziff [6] have found $\Omega = 0.64 \pm 0.02$ at $p = p_c$ from Monte Carlo simulations of bond percolation on different cubic lattices. Note, however, that the internal cut-off function obtained from simulations is not relevant for comparison with real systems because the internal cut-off function is system dependent.

On the other hand, knowledge of the external cut-off function at finite ε is very important for any application of the percolation model to real systems. The external cut-off has been investigated by Hoshen *et al* [11] and more recently by Stauffer [14]. In these simulations a normalized external cut-off function was calculated in terms of the parameter $X = \varepsilon s^\sigma$ at different values of ε as

$$f_{\text{ext}}(X, \varepsilon, L) = \frac{N(s, \varepsilon, L)}{N(s, 0, L)}. \tag{7}$$

We have made explicit in equation (7) the dependence on the lattice size L and ε in order to stress that finite size effects on f_{ext} need to be considered even if f_{ext} is calculated by normalization with the size distributon at $\varepsilon = 0$ and the same lattice size. It was assumed in [11, 14] that using equation (7) finite size effects on the external cut-off function are simply divided out and are no longer important. The authors concluded that $f_{\text{ext}}(X, \varepsilon, L)$ was a function only of X and could be described by a Gaussian with the maximum situated at $X > 0$. They also found that within the statistical error f_{ext} does not depend on the detail of the lattice.

Figure 4 shows $N(s, \varepsilon, \infty)/N(s, 0, \infty)$ as a function of $X = \varepsilon s^\sigma$ for different values of ε, both for p smaller and larger than p_c. We used the literature value $\sigma = 0.45$, which resulted in good superposition of the data at different ε. In figure 4 all the data superimpose even for small s, which implies that the internal cut-off function does not depend on ε. The solid line in figure 4(a) shows that the data can be approximated by a Gaussian. However, a semi-logarithmic representation shows that for $p > p_c$ the data are better described by a

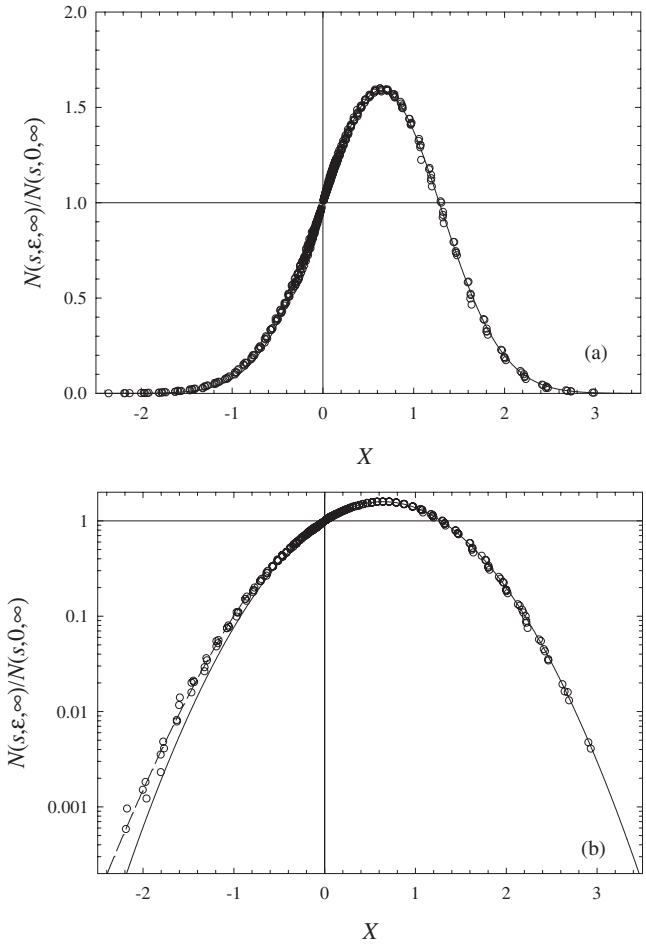

Figure 4. Linear (a) and semi-logarithmic (b) representations of the cut-off function of the normalized size distribution as a function of $X = \varepsilon\, s^{\sigma}$. The data are the same as shown in figure 2 with $|\varepsilon| \leqslant 4.5 \times 10^{-2}$. The solid lines represent equation (8) and the dashed line represents equation (9).

stretched exponential, see the dashed line in figure 4(b). Nonlinear least squares fits give

$$f_{\mathrm{ext}}(X) = 1.589 \pm 0.004 \exp\left[-\frac{1}{2}\left(\frac{X - 0.641 \pm 0.002}{0.666 \pm 0.002}\right)^2\right] \qquad X > 0 \tag{8}$$

$$f_{\mathrm{ext}}(X) = \exp\left(-2.3 \pm 0.1\,|X|^{1.5\pm0.1}\right) \qquad X < 0. \tag{9}$$

The errors represent again the 95% confident interval. Note that the prefactor of equation (8) is not a fit parameter, but was chosen such that $f_{\mathrm{ext}}(0) = 1$. Kunz and Souillard [15, 16] derived the limiting behaviour of $N(s)$ for $|X| \gg 1$: $\log N(s) \propto X^{\zeta}$ with $\zeta = 1/\sigma = 2.22$ for $X > 0$ and $\zeta = 2/(3\,\sigma) = 1.48$ for $X < 0$, where we use again $\sigma = 0.45$. It is difficult to obtain data at $|X| > 1$ with high accuracy, but the results shown in figure 4 are, at least, compatible with these predictions.

In figure 5(a) we have plotted the size distributions at $\varepsilon = 0$ for different values of L. The distribution extrapolated to $L \to \infty$ is represented by the dashed line. For $\varepsilon = 0$ the cut-off

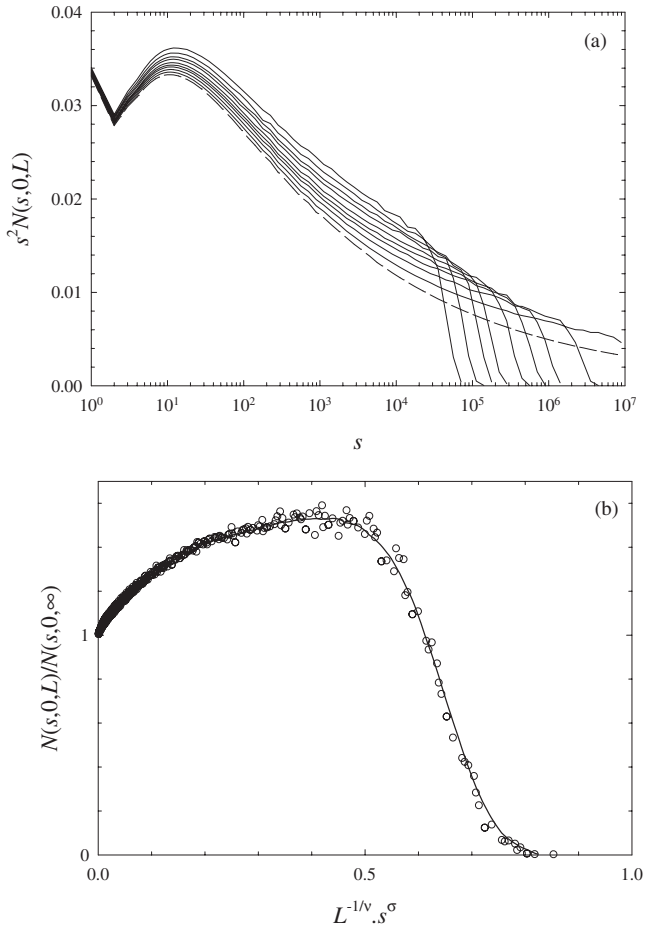

Figure 5. (*a*) Evolution of $s^2\,N(s, 0, L)$ as a function of s at various L: 102, 124, 150, 174, 222, 276, 342, 511 and 1023. The dashed line represents the extrapolation at $L = \infty$. (*b*) Normalized size distribution at the percolation threshold using the data shown in figure 5(*a*). The solid line represents a smooth interpolation of the data.

function is fully determined by the finite extent of the lattice at a characteristic size proportional to $L^{1/D}$. In figure 5(*b*) we have plotted $N(s, 0, L)/N(s, 0, \infty)$ as a function of $s^{\sigma}\,L^{-1/\nu}$ for different values of L, where $\nu = \sigma\,D = 0.88$. We did not find a simple analytical function to describe the cut-off function at $\varepsilon = 0$ and in the following we use for $N(s, 0, L)/N(s, 0, \infty)$ the solid line in figure 5(*b*) which represents a smooth interpolation of the data uninfluenced by the internal cut-off.

Having established the cut-off functions of the size distribution at $L \to \infty$ for finite values of ε and at $\varepsilon = 0$ for finite values of L, we are in a position to evaluate the cut-off functions at finite values of L and $\varepsilon \neq 0$. We limit ourselves to the case $p < p_c$ ($\varepsilon > 0$). In figure 6 we show $f_{\text{ext}}(X, \varepsilon, L)$ for different values of ε and L considering only large values of L and small values of ε. Clearly $f_{\text{ext}}(X, \varepsilon, L)$ is not independent of ε and L. The neglect of this dependence explains the large noise in the data presented in [11, 14] where results obtained at different ε and L were assumed to describe a unique function. In fact $f_{\text{ext}}(X, \varepsilon, L)$ is a function of the parameter $Y = \varepsilon\,L^{1/\nu}$. Since the radius ($R^*$) of the cluster with size s^* varies

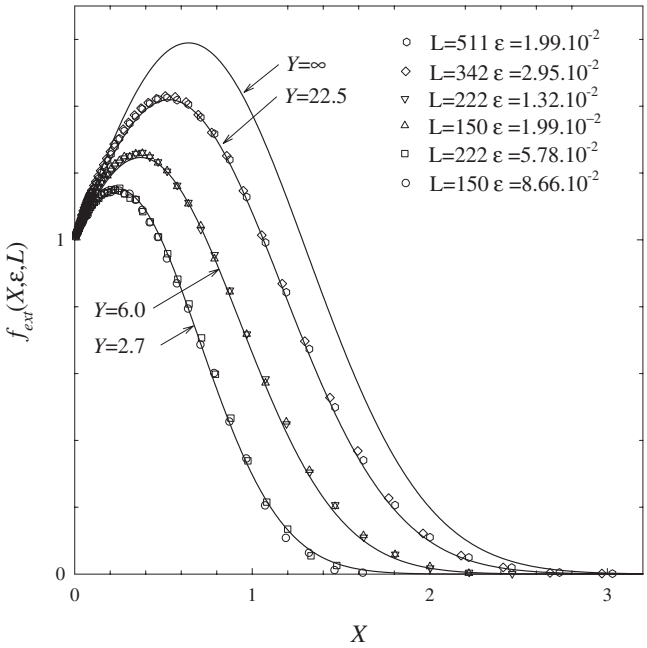

Figure 6. External cut-off function of the size distribution for different couples (ε, L) corresponding to three different values of $Y = \varepsilon L^{1/\nu}$ as indicated in the figure. For comparison, we also show the result for $Y = \infty$ (equation (8)).

as $R^* \propto \varepsilon^{-\nu}$ it follows that $Y \propto (L/R^*)^{1/\nu}$. The cut-off function, $f_{\text{ext}}(X, Y)$, is well described by a Gaussian, but with parameters that are a function of Y. For $X \geqslant 0$ and $Y \geqslant 0$ we have

$$f_{\text{ext}}(X, Y) = A(Y) \exp\left[-\frac{1}{2}\left(\frac{X - X_0(Y)}{B(Y)}\right)^2\right] \tag{10}$$

with

$$A(Y) = \exp\left[\frac{1}{2}\left(\frac{X_0(Y)}{B(Y)}\right)^2\right]. \tag{11}$$

The dependence of the parameters X_0 and B on Y is shown in figure 7 and is in both cases well described by the following analytical functions:

$$X_0(Y) = \frac{0.641}{\left(1 + (a/Y)^b\right)^c} \tag{12}$$

$$B(Y) = \frac{0.666}{(1 + (d/Y)^e)^f}. \tag{13}$$

A nonlinear least squares fit gave for the parameter X_0: $a = 4.0 \pm 0.6$, $b = 0.95 \pm 0.02$ and $c = 1.1 \pm 0.1$. While for the parameter B we obtained $d = 1.4 \pm 0.2$, $e = 1.05 \pm 0.02$ and $f = 0.9 \pm 0.1$. Note that for $L \to \infty$ we recover equation (8).

We can write the full expression for the size distribution as a universal function of the parameters X and Y by combining the equations (2), (6), (7) and (10):

$$N(s, \varepsilon, L) = k_1 s^{-\tau} (1 + k_2 s^{-\Omega}) f_{\text{ext}}(X, Y) g(X/Y). \tag{14}$$

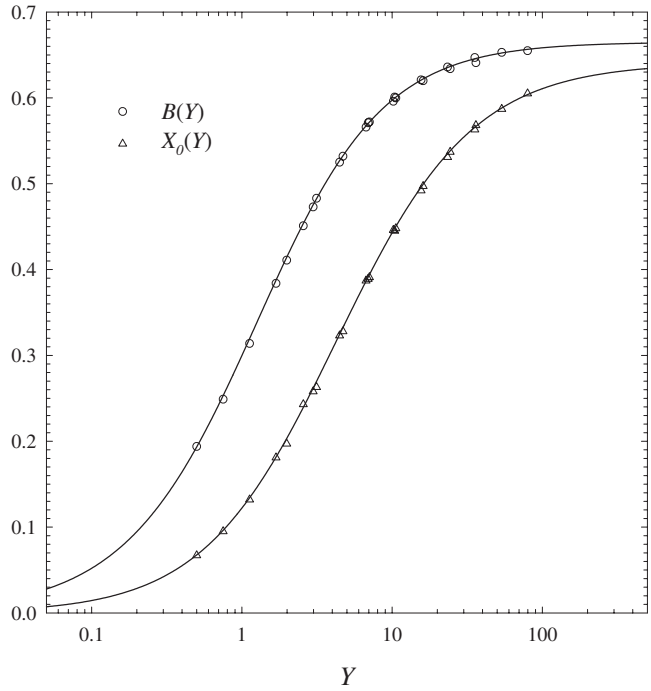

Figure 7. Dependence of the parameters in equation (10) on Y. The solid lines correspond to the fits using equation (12) and (13).

Here $g(X/Y)$ is the external cut-off function at $\varepsilon = 0$ indicated by the solid line in figure 5(b) noting that $X/Y = s^{\sigma} L^{-1/\nu}$. This expression is valid for any L sufficiently large and ε sufficiently small.

In the simulations we have calculated the weight average (s_{w}) and z-average (s_z) sizes. In the limit of $L \to \infty$ and for ε sufficiently small, s_z and s_{w} have a power law dependence on ε: $s_z \propto |\varepsilon|^{-1/\sigma}$ and $s_w \propto |\varepsilon|^{-\gamma}$ with $\gamma = (3 - \tau)/\sigma = 1.80$. In figures 8 and 9 we have plotted $s_z\, \varepsilon^{1/\sigma}$ and $s_w\, \varepsilon^{\gamma}$ as a function of Y using results at $0 < \varepsilon \leqslant 4.5 \times 10^{-2}$ and $L \geqslant 150$. Good superposition of the data at different ε is obtained if we chose the literature values of σ, γ and ν. As expected finite size effects on s_z and s_{w} are a universal function of $Y = \varepsilon\, L^{1/\nu}$. For $Y \to \infty$, $s_z\, \varepsilon^{1/\sigma}$ and $s_w\, \varepsilon^{\gamma}$ become constant while for $Y \to 0$ we find that $s_z\, \varepsilon^{1/\sigma} \propto Y^{1/\sigma}$ and $s_w\, \varepsilon^{\gamma} \propto Y^{\gamma}$. We can calculate the finite size effects on s_z and s_{w} explicitly using equation (11) in equations (4) and (5), see solid lines in figures 8 and 9. The agreement between the simulated and calculated values is satisfactory and shows that equation (14) is a good description of the size distribution over the whole range of $\varepsilon\, L^{1/\nu}$, provided that ε is sufficiently small ($0 < \varepsilon \leqslant 4.5 \times 10^{-2}$) and L is sufficiently large ($L \geqslant 150$).

3. Conclusions

- Finite lattice size effects on the size distribution of percolating clusters on cubic lattices are a universal function of $\varepsilon\, L^{1/\nu}$.
- For $s \geqslant 10$ the internal cut-off function can be described by

$$f_{\mathrm{int}}(s) = 0.0690\,(1 - 1.13\, s^{-0.65}) \tag{15}$$

for ε sufficiently small.

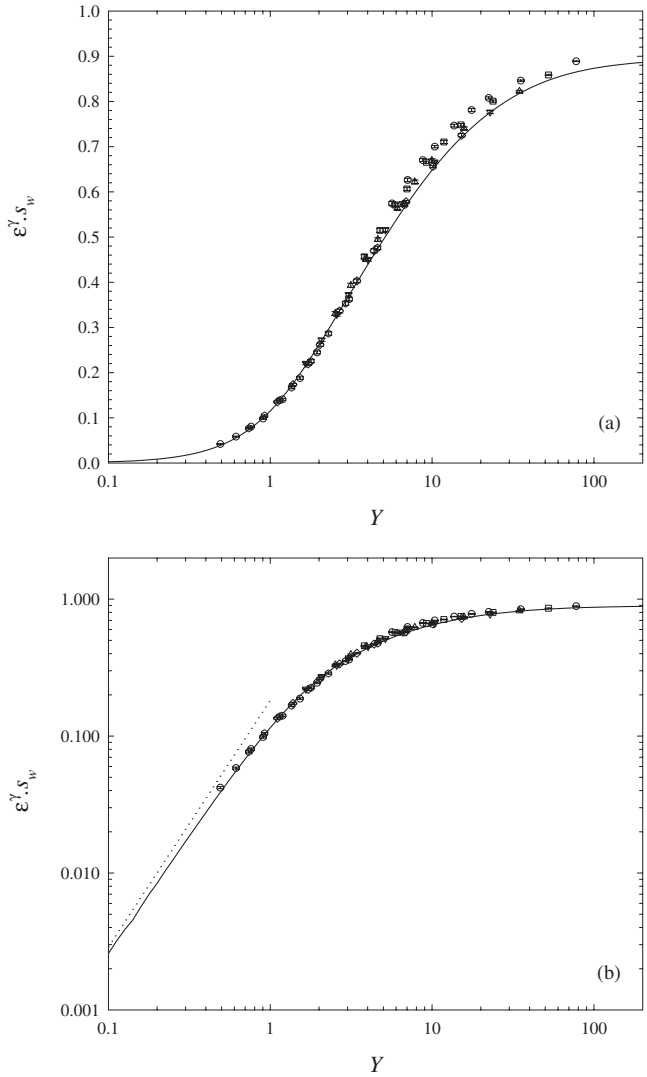

Figure 8. Semi-logarithmic (*a*) and double-logarithmic (*b*) representations of the finite size effects on s_w using $\gamma = 1.80$. The solid lines were obtained using equations (4) and (14). The dashed line represents the asymptotic behaviour at $Y \to 0$. The error bars represent confidence intervals of 95%.

- The external cut-off function of $N(s)$ at $\varepsilon > 0$ cannot be obtained by normalizing $N(s)$ with the size distribution at $\varepsilon = 0$. External cut-off functions of the normalized size distributions do have a Gaussian form, but with parameters that depend on $\varepsilon L^{1/\nu}$. Only by extrapolation to $\varepsilon L^{1/\nu} \to \infty$ can the true external cut-off function of $N(s)$ be obtained.
- Finite size effects of the weight averaged and z-averaged size of the clusters can be calculated explicitly using the external cut-off functions of the normalized size distributions.
- The external cut-off function of $N(s)$ at $p > p_c$ is better described by a stretched exponential than a Gaussian function.

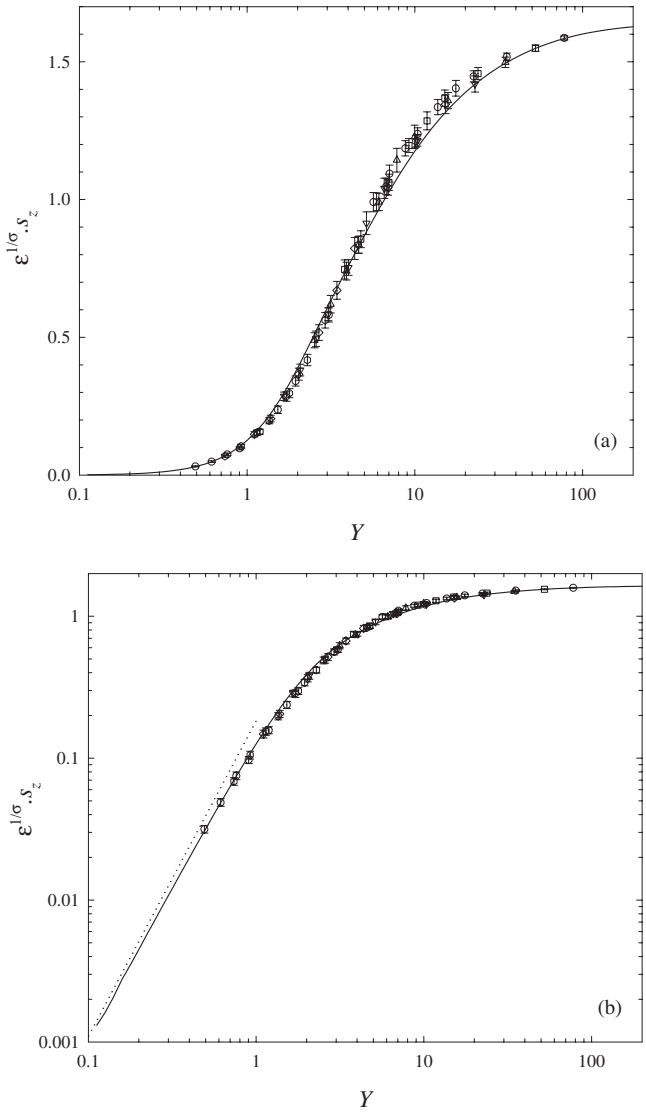

Figure 9. Semi-logarithmic (*a*) and double-logarithmic (*b*) representations of the finite size effects on s_z using $\sigma = 0.45$. The solid lines were obtained using equations (5) and (14). The dashed line represents the asymptotic behaviour at $Y \to 0$. The error bars represent confidence intervals of 95%.

References

[1] de Gennes P-G 1979 *Scaling Concepts in Polymer Chemistry* (Ithica, NY: Cornell University Press)
[2] Stauffer D and Aharony A 1992 *Introduction to Percolation Theory* 2nd edn (London: Taylor & Francis)
[3] Ziff R and Stell G 1988 Laboratory for Scientific Computing of College of Engineering, Report No. 88-4, University of Michigan (unpublished)
[4] Grassberger P 1992 *J. Phys. A: Math. Gen.* **25** 5867.
[5] Jan N and Stauffer D 1998 *Int. J. Mod. Phys.* C **9** 341
[6] Lorenz C D and Ziff R M 1998 *Phys. Rev.* E **57** 230
[7] Nicolai T, Durand D and Gimel J C 1994 *Phys. Rev.* B **50** 16357

[8] Gimel J C, Nicolai T, Durand D and Teuler J M 1999 *Eur. Phys. J.* B **12** 91
[9] Hoshen J and Kopelman R 1976 *Phys. Rev.* B **14** 3438
[10] Margolina A, Nakanishi H, Stauffer D and Stanley H E 1984 *J. Phys. A: Math. Gen.* **17** 1683
[11] Hoshen J, Stauffer D, Bishop G H, Harrison R J and Quinn G D 1979 *J. Phys. A: Math. Gen.* **12** 1285
[12] Sykes M F, Gaunt D S and Glen M 1976 *J. Phys. A: Math. Gen.* **9** 1705
[13] Mertens S 1990 *J. Stat. Phys.* **58** 1095
[14] Stauffer D 1986 *On Growth and Form. Fractal to Non-Fractal Patterns in Physics* ed H E Stanley and N Ostrowski (Boston: Martin Nijhoff) p 79
[15] Kunz H and Souillard B 1978 *Phys. Rev. Lett.* **40** 133
[16] Kunz H and Souillard B 1978 *J. Stat. Phys.* **19** 77